Automated Quantification of the Effects of Low Body Negative Pressure on Left Ventricular Function during Parabolic Flight

C Corsi[1], P Vaida[2], EG Caiani[3]

[1]D.E.I.S. - University of Bologna, Italy
[2]Université Bordeaux 2, Médecine Aérospatiale, Bordeaux, France
[3]Politecnico di Milano, Dipartimento di Bioingegneria, Milano, Italy

Abstract

To study modifications in left ventricular (LV) dimensions induced by gravitational stresses, and evaluate the effects due to lower body negative pressure (LBNP) countermeasure, we performed 2D echocardiographic imaging during parabolic flights on a group of eleven subjects (mean age ± SD, 46 ± 5 years) in upright position with and without LBNP applied. To detect LV endocardial contours, a semi-automatic procedure based on level set methods was applied. The analysis was performed both averaging four consecutive end diastolic (ED) and end systolic (ES) frames, and frame by frame in a cardiac cycle, allowing the computation of ED (EDA) and ES (ESA) areas and LV area over time. Modifications in LV dimensions according to different gravity conditions were found: a LV dilation was observed during 0 Gz, preceded by its contraction during 2 Gz. When LBNP was applied, it appeared effective in reducing venous return and minimizing LV dilation.

1. Introduction

Microgravity is the only laboratory condition which can give better insight in processes that are influenced by gravity at a cellular and organism level. Although the microgravity period during parabolic flights last only 20-25 seconds, it is in some cases enough to investigate the effect of gravity on cardiovascular system. It is known that modifications in gravity level (head-to-foot acceleration, Gz) cause shifts in fluid from the lower extremities toward the head and thorax, altering central filling volumes and pressures, resulting in significant cardiovascular effects [1-2]. These modifications, together with changes in the sympathetic activity (heart rate and inotropic status), influence left ventricular (LV) dimensions and function. These hemodynamic alterations are responsible for many of the consequences associated with post-flight orthostatic intolerance in astronauts [3]. Therefore, the evaluation of these changes is important for the definition and testing of appropriate countermeasures to balance the effects of weightlessness on the cardiovascular system, as well as for the better understanding of the human physiology. Among them, low body negative pressure (LBNP) is a countermeasure that acts in order to reduce venous return.

Echocardiography is a noninvasive, widespread and powerful diagnostic tool and because of its portability it can be utilized during parabolic flights. Visualizing the heart chambers in real-time, this imaging technique allows us to follow their modification in size induced by different gravitational stresses and determine countermeasure effectiveness.

The application of image processing procedures to automatically detect endocardial boundaries and compute LV dimensions could speed up the data analysis and reduce the variability in the results due to subjective interpretations.

Aim of this study was to evaluate the effectiveness of LBNP on reducing venous return during parabolic flight by studying the modifications in LV area under different gravity conditions, by means of a procedure, based on level-set methods, to automatically trace the LV endocardial boundaries.

2. Method

2.1. Experimental protocol

Parabolic flights were performed in the Zero-G Airbus A-300, managed by Novespace for CNES and ESA in Bordeaux, France. A flight campaign consists in three days of flight, each lasting about 3 hours and consisting of 31 parabolas. Each parabola included four consecutive phases: normogravity (1 Gz), before the parabola begun; mild hypergravity (1.8 Gz) during the ascending phase of the parabola, microgravity (0 Gz) lasting for about 20s; a second period of mild hypergravity (1.8 Gz) during the descending phase of the parabola (20-25 s), followed by a new steady state at 1 Gz (1 min). A group of eleven healthy subjects (mean age ± SD, 46 ± 5 years) was studied in standing upright position with their abdomen and legs enclosed in a LBNP chamber. Ultrasound images (Aspen, Acuson, France Siemens, France) were continuously obtained, with a frame rate between 20 and 37 Hz, from the apical 4-chamber view and saved onto a magneto-optical disk. For each subject, a LBNP of -50 mmHg was randomly applied during 0 Gz in half of the parabolas. For the analysis, good image quality data obtained from one parabola without LBNP and one parabola with LBNP applied during 0 Gz were selected.

2.2. Level set method

To detect endocardial contours, a semi-automatic procedure based on level set methods was developed. Level set methods are numerical techniques used to track the evolution of interfaces [4], which have been applied to edge detection, shape recovery, representation and recognition in a medical imaging environment.

The level set approach is an implicit representation of curves, in the form of a partial differential equation that tracks boundaries as they evolve in space and time. The basic idea behind the level set methodology is to embed a propagating front as the zero level set of a higher dimensional, Lipschitz and continuous function. Let's consider a 2D space and a curve $\gamma(t)$ that is propagating under the speed F in the normal direction: F indicates how to move each point of the curve. Instead of following the curve itself the original curve is built into a surface that intersects the *xy* plane exactly where the curve sits. The graph of the surface is the *level set function* because it accepts as input any point in the plane and hands back its height as output; the intersection with the *xy* plane is called *zero level set* because it is the set of points that are at height zero. To move the front the level set function is changed instead of moving the initial curve. The curve represents the moving zero level set of the level set function. A partial differential equation describes the evolution of the level set function $\varphi(\mathbf{x},t)$:

$$\frac{\partial \varphi}{\partial t} + F|\nabla \varphi| = 0$$

with the initial condition $\varphi(\mathbf{x},t) = \varphi_0$ and F a defined speed function. In the application of level set models for image analysis the speed function used to control shape recovery process in the image $I(\mathbf{x})$ is:

$$F = g\varepsilon K - \beta \nabla g \cdot \frac{\nabla \varphi}{|\nabla \varphi|}$$

with

$$g(x) = \frac{1}{1 + \left(\frac{|\nabla G_\sigma * I(x)|}{\alpha} \right)^2} \qquad G_\sigma(\xi) = \left(1/\sigma\sqrt{\pi}\right) e^{-(\xi/\sigma)^2}$$

In the expression of F the first term is a curve tension force that depends on the Euclidean curvature K and the second term is a force that attracts the curve towards the boundaries and thus has a stabilizing effect. The edge indicator g, is a non-increasing function of the gradient of a smoothed version of the initial image [5].

The parameters α and σ depend on the characteristics of the noise in the image: α selects the contrast of the objects to consider in the image during the motion of the embedding, and σ is the variance of the Gaussian determined by the size of the smallest features we desire to detect. The parameter β is used to limit the regularization of the embedding controlled by the parameter ε.

The resulting equation of motion for the level set function is:

$$\frac{\partial \varphi}{\partial t} + g\varepsilon K|\nabla \varphi| - \beta \nabla \varphi = 0$$

The curve evolution will have a steady state solution when the geometry dependent term balances the advection term. The initial curve is user-defined, and when analyzing a cine-loop, this initialization is required for the first frame only because the procedure takes the estimated contour of the previous frame as initial condition for the contour detection of the following frame.

2.3. Data analysis

To take into account respiratory changes in venous return, for each gravity phase (1Gz, 1.8 Gz and 0 Gz) in each experimental condition (without and with LBNP) four consecutive end diastolic (ED) and end systolic (ES) frames were selected and analyzed by level set method, and their mean ES and ED areas computed. The reliability of the contour identification was assessed by visual inspection by an expert operator, by superimposing the detected contours on the original images.

Moreover, in a subgroup of nine subjects, images obtained during a whole cardiac cycle were selected and the analysis performed frame-by-frame to allow the computation of LV area over time. ED and ES areas (EDA and ESA respectively), together with FAC (fractional area change as EDA-ESA) and FAC% (as FAC/EDA·100) were computed. By a cubic spline interpolation, the LV area versus time curve was fitted to increase time resolution and to compute its first derivative. Then, the following parameters were semi-automatically extracted: heart beat duration (RR), systolic phase duration (tSYS), diastolic phase duration (tDIA), peak ejection (PER), peak filling (PFR), peak atrial filling (PAFR) rate. A two-way analysis of variance was applied (F-test significant for $p<0.05$) to test the effects of different gravity on LV dimension and to verify if the application of LBNP would have any significant consequence on LV size and function.

3. Results

The proposed method was able to detect reliable LV endocardial contours in all the analyzed frames. An example of the detected contours superimposed to the original images of the same subject, during 0 Gz phase without and with LBNP applied is shown in figure 1.

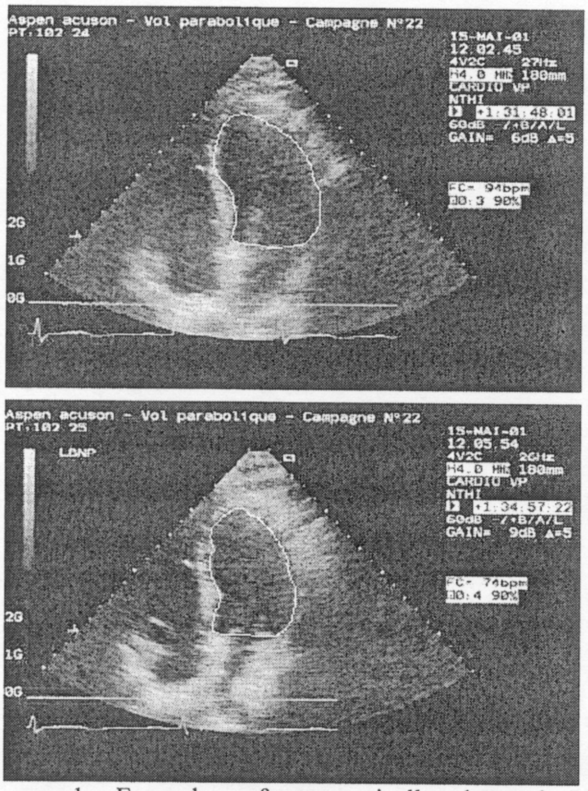

Figure 1. Examples of automatically detected LV endocardial contours superimposed to the original images at 0 Gz without (up) and with LBNP applied (bottom).

The analysis of averaged ED and ES areas showed modifications in LV dimensions according to different gravity conditions. Compared to 1 Gz values, at 1.8 Gz EDA and ESA were significantly reduced of 8.8±6.1% ($p<0.01$) and 10.3±8.5% ($p<0.01$) respectively (see Figure 2). During 0 Gz, when LBNP was not applied EDA and ESA were increased by 15.8±5.8% and 12.3±7.0% respectively in respect to 1 Gz. On the contrary, when LBNP was applied, EDA and ESA were increased of only 8.9±5.6% and 8.2±7.7% respectively.

Moreover, comparing LV dimensions during 0 Gz with and without LBNP, significant changes were found: with LBNP applied, EDA and ESA areas were respectively reduced of 9.5±7.6% ($p<0.01$) and 10.3±3.7% ($p<0.01$) compared with their values without LBNP applied.

The frame-by-frame analysis of the whole cardiac cycle allowed us to obtain LV area curves over time, an example of which is shown in figure 3. The curve was

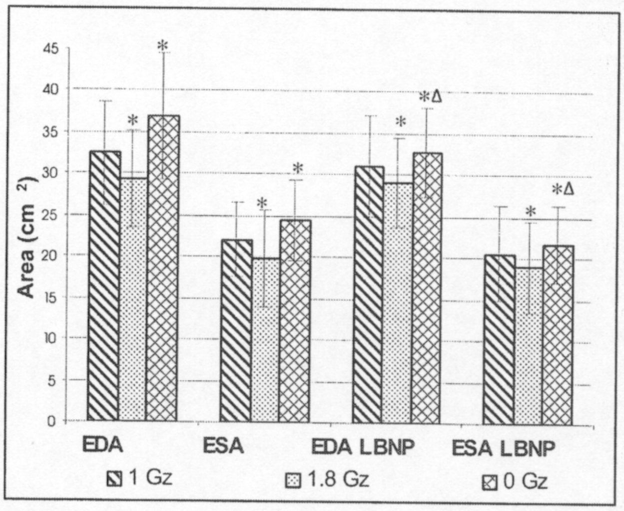

Figure 2. Averaged values of EDA and ESA (mean±SD) during the different gravity phases, without and with the LBNP countermeasure applied (* significant respect to 1 Gz value; Δ significant respect to 0 Gz value without LBNP applied).

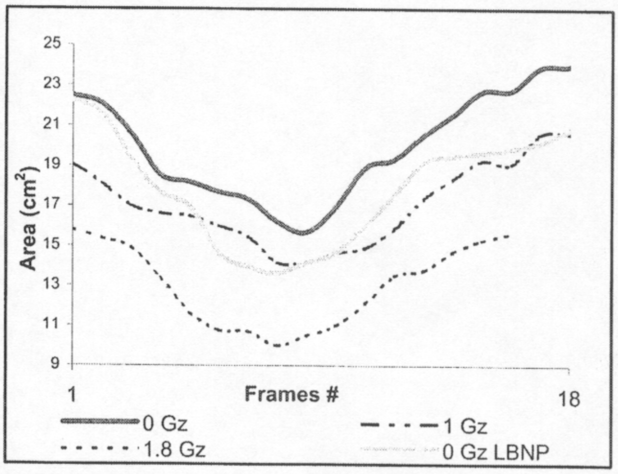

Figure 3. LV area over time at 1 Gz, 1.8 Gz, 0 Gz without LBNP and with LBNP applied.

shifted towards lower and higher values of area at 1.8 Gz and 0 Gz respectively, compared to 1 Gz. On the contrary, with LBNP applied, the curve at 0 Gz appeared to be quite similar to the normogravity condition.

In table I the mean values of the parameters of LV function extracted from the LV area curves are reported, confirming previous observations on LV dimensions.

4. Discussion

Despite the not optimal quality of the images, due to the experimental conditions, the proposed algorithm was able to reliably detect the LV endocardial boundaries.

Expected modifications in LV area were found, related both to the experimental condition and the gravity level.

Due to abrupt changes in venous return, a LV

Table 1. Mean values ± SD dev. of the computed parameters during the three gravity phases, without and with LBNP.

	1 Gz	1.8 Gz	0 Gz	0 Gz LBNP
EDA (cm^2)	32.42 ± 6.16	29.33 ± 5.90*,**	36.91 ± 7.65°	32.81 ± 5.36°°
ESA (cm^2)	22.10 ± 4.56	19.83 ± 5.84*,**	24.55 ± 4.92*	21.70 ± 4.61°°
FAC (cm^2)	10.32 ± 2.88	9.49 ± 3.73^	12.36 ± 4.07	11.11 ± 1.56
FAC%	31.6 ± 6.2	32.8 ± 11.3	33.1 ± 6.2	34.27 ± 4.92
RR (ms)	598.5 ± 112.0	532.1 ± 100.2^	613.8 ± 107.2	713.1 ± 290.8^
tSYS (ms)	274.2 ± 62.0	245.9 ± 57.2	267.8 ± 62.0	283.3 ± 80.3
tDIA (ms)	324.3 ± 97.2	286.2 ± 66.2	346.0 ± 87.6	429.8 ± 73.3^
PER (cm^2/s)	-29.9 ± 9.4	-27.2 ± 10.9	-35.0 ± 16.2	-31.2 ± 11.4
PFR (cm^2/s)	26.2 ± 9.2	22.4 ± 7.0^	31.7 ± 6.6	23.4 ± 8.0
PAFR (cm^2/s)	17.5 ± 6.1	16.0 ± 12.3	19.1 ± 10.3	17.9 ± 7.8

*$p<0.05$ vs 1 Gz; °$p<0.01$ vs 1 Gz; **$p<0.01$ 1.8 Gz vs 0 Gz; ^$p<0.05$ 1.8 Gz vs 0 Gz ; °° $p<0.01$ 0 Gz vs 0 Gz with LBNP.

chamber dilation was observed during 0 Gz, preceded by its contraction during 1.8 Gz. In fact, during hypergravity the blood is maintained in the lower part of the body, while in microgravity it tends to accumulate in the head and the torax. The application of the LBNP countermeasure, trying to maintain the blood in the legs by means of a negative pressure, showed its effectiveness by reducing the increase in LV sizes, compared to the results obtained without LBNP: indeed, LBNP application during 0 Gz significantly contributed in the reduction of the LV area, not only in telesystole and telediastole but during the entire cardiac cycle. In fact, the analysis of LV area extended to the whole cardiac cycle, instead of being limited to the telediastolic and telesysolic frames, allowed to quantify the dynamic changes in LV area during the cardiac cycle and to extract several LV function parameters.

5. Conclusion

The results of this study confirmed that different gravity phases of a parabolic flight sequence could generate acute changes in venous return and cardiac loading conditions. The LBNP, applied as a countermeasure during the microgravity phase to partly counteract fluid shift from the lower part of the body, appeared effective in reducing the LV dilation by decreasing the venous return.

Acknowledgements

We would like to thank Dr. O. Bailliart, Dr. B. Cholley and Dr. A. Capderou for their help in carrying out the experiments and collecting data, and Prof. C. Lamberti and Prof. S. Cerutti for their support.

References

[1] Mukai CN, Lathers C.M, Charles JB, Bennet BS. Cardiovascular responses to repetitive exposure to hyper- and hypogravity states produced by parabolic flights. J Clin Pharmacol 1994;34:472-9.

[2] Lathers CM, Charles JB, Elton KF, Holt TA, Mukai C, Bennet BS, Bungo MW. Acute hemodynamic responses to weightlessness in humans. J Clin Pharmacol 1989;29:615-27.

[3] Guell A, Braak L. Cardiovascular deconditioning syndrome during space flight. Ann Cardiol Angiol 1989;38(8):499-502.

[4] Osher S, Sethian JA. Fronts Propagating with Curvature Dependent Speed: Algorithms Based on Hamilton Jacobi formulation. J Comp Physics 1988;79: 12-49.

[5] Perona P, Malik J. Scale-space and Edge Detection using Anisotropic Diffusion. IEEE Trans on Pattern Analysis and Machine Intelligence1990;12:629-639.

Address for correspondence:

Cristiana Corsi
DEIS, Università degli Studi di Bologna
Viale Risorgimento 2, 40136 Bologna, Italy.
E-mail: ccorsi@deis.unibo.it